Physica A 161 (1989) 249–268
North-Holland, Amsterdam

CLUSTERS IN THE THREE-DIMENSIONAL ISING MODEL WITH A MAGNETIC FIELD

Jian-Sheng WANG
HLRZ, c/o Kernforschungsanlage Jülich, Postfach 1913, D-5170 Jülich 1, Fed. Rep. Germany

Received 2 July 1989

We study the clusters generated in the Swendsen–Wang algorithm in a magnetic field. It is shown that the number of clusters is related to that of Coniglio and Klein by simple factors. With this definition of clusters, infinite size appears whenever the system has a nonzero magnetization. Scaling behavior of the number of clusters near the critical point is confirmed. The number of clusters away from the critical point for large cluster size s is consistent with $\ln n_s \simeq -|h|s - \Gamma s^{2/3}$ on the low temperature side of the Coniglio–Klein cluster percolation transition line, and is consistent with $\ln n_s \simeq -(|h| + c)s$ on the high temperature side. We also argue that this transition line is given by $h = \pm\tilde{h}(T) \propto (T - T_c)^{1/\sigma}$ near T_c.

1. Introduction

The study of the phase transition or condensation process of a gas into a liquid in terms of clusters started very early. Mayer's cluster expansion [1] can be considered as an early study for equilibrium. Explicit use of physical clusters, namely, a group of molecules very close to each other, appeared in a "droplet" model of Band and his Chinese collaborators [2]. Fisher extended the droplet model to the critical point [3, 4]. Subsequently, various modifications of the Fisher droplet model were undertaken [5]. In the simplest version of semi-phenomenological models, a vapor system is considered as noninteracting droplets of liquid of various sizes. One assumes that the free energy divided by $k_B T$ of a droplet with s molecules has a bulk term hs ($h = 2H/k_B T$ in the Ising spin language) and a surface term Γs^{σ} ($\Gamma = \text{const} \times |T - T_c|$), where a renormalized surface area s^{σ} is used instead of $s^{2/3}$ as at low temperatures. The number of clusters having size s is supposed to be

$$n_s \propto s^{-\tau} e^{-hs - \Gamma s^{\sigma}}. \tag{1}$$

This assumption leads to scaling relations among critical exponents [3]. The cluster number is also an important ingredient in nucleation theory [6].

0378-4371/89/$03.50

The question that arises naturally is how to define droplets in a microscopic model. Let us consider the Ising model, or lattice gas, which associates a "+" spin in the magnet with the absence of an atom in the gas and a "−" spin with the presence of an atom. What is called Ising clusters is a first candidate for the droplets. The Ising clusters (or geometric clusters) are sets of sites with Ising spins "−" connected to nearest neighbors which are also "−". This is the definition of clusters used in early studies [7–10]. We take the case where most spins are "+". At low temperatures such "−" spin clusters are small and compact. As temperature rises, bigger clusters appear. Eventually, an infinitely large cluster is formed. This, it turns out, occurs below the critical temperature of the second-order ferromagnetic phase transition for dimensions $d > 2$ [7, 11]. Thus the identification of the thermal phase transition as a geometric percolation transition [12] with the same set of critical exponents is not achieved using Ising clusters. The cluster numbers can not be described by the Fisher droplet model, eq. (1), or more generally, its scaling structure [9].

In two dimensions, although the percolation transition coincides with the thermal phase transition due to topological reasons [13], the critical behavior is not the same [14, 15]. It was realized that the Ising clusters are too compact for thermal phase transitions [16]. A correct cluster definition, which gives the thermodynamic phase transition, should be a subset of those Ising clusters. It is remarkable that a simple procedure exists for this purpose. Coniglio and Klein [13] show that if the Ising clusters were cut, with a probability e^{-2K} ($K = J/k_B T$) between bonds of "−" spins, so that the original cluster might fall into pieces, the resulting clusters give exactly the desired properties: the percolation transition of the clusters occurs at the critical temperature; percolation critical exponents are identical to the thermal critical exponents. We shall refer to these clusters as CK clusters in the following. The reason behind this successful identification of the percolation cluster transition (in zero field) with the thermodynamic phase transition is due to a mapping between the Ising model (or more generally, Potts models) and a type of correlated percolation problems [17, 18]. The same mapping has led to an algorithm [19] to be discussed in the next section with considerably faster dynamics.

If we want a complete description of the thermal phase transition by cluster percolation, the CK clusters have a drawback: using the cluster definition of Coniglio and Klein in a magnetic field, a line of percolation transitions occurs which starts from the critical point and ends at infinite negative field and at a temperature corresponding to a random bond percolation threshold [20, 11]. (We take the convention that CK clusters are built from "−" spins.) This problem also occurs in the work of Hu [18]; we refer to Kertész [22] for further discussion. This transition line can be "removed" if we consider the clusters generated in the Swendsen–Wang (SW) algorithm with a ghost spin [19]. Due

to the ghost spin, there will always be an infinite-size cluster whenever the system has a non-zero magnetic field. With this new definition of clusters, the percolation phase diagram is identical to the thermal phase diagram. In this article we show some properties of such clusters and their relations with clusters of Coniglio and Klein. We then report our extensive Monte Carlo calculation of cluster size distribution, using the method of cluster updating of Swendsen and Wang.

2. SW algorithm

We shall just state the SW algorithm. Its justification [19, 23] and generalizations can be found in the literature [24–29].

To fix our notation, let us write the Ising Hamiltonian as

$$H = -K \sum_{\langle i,j \rangle} (\sigma_i \sigma_j - 1) - \tfrac{1}{2} h \sum_i \sigma_i , \tag{2}$$

where site i is on a d-dimensional hypercubic lattice of linear size L. The first summation is over nearest-neighbor pairs, $K = J/k_B T > 0$, $h = 2H/k_B T$, and $\sigma_i = \pm 1$. The partition function is

$$Z = \sum_{\sigma} e^{-H} . \tag{3}$$

We have deliberately added a configuration-independent term KdL^d, so that each pair of interactions in the partition function can be written as $e^{K(\sigma_i \sigma_j - 1)} = (1-p) + p\delta_{\sigma_i,\sigma_j}$; here $p = 1 - e^{-2K}$. Thus an expansion in terms of clusters is achieved [17, 18].

The SW algorithm in zero field goes as follows:

(1) From a spin configuration one lays down bonds between pairs of nearest neighbors with a probability p if the nearest neighbor spins are parallel. No bonds shall be present if the spins have opposite signs.

(2) After each pair of interactions is treated by step (1), clusters are identified. A cluster may consist of one site, or more sites connected through bonds.

(3) An up or down orientation of spins is chosen with equal probability for each cluster. All its sites in the cluster receive the same new spin. Thus a new configuration is generated. We then go back to step (1).

When there is a magnetic field, two versions of the algorithm exits [19]: with or without a ghost spin. We first state the algorithm without a ghost spin. Modification to the above algorithm is in assigning spins to clusters (step (3)).

Each cluster is like a noninteracting Ising spin experiencing a field of strength $hs_\alpha/2$, where s_α is the size of cluster α. Spin η_α for the cluster α is sampled according to probability $\exp\{hs_\alpha \eta_\alpha/2\}$.

The second version utilizes the ghost spin [17]. Modification to the zero field case is in generating bonds. We formally write the field term $\frac{1}{2}h\sigma_i$ as $\frac{1}{2}|h|\sigma_i\sigma_g$, where σ_g is so-called ghost spin which takes the value $\mathrm{sgn}(h)$ and does not change. Now the field term looks just the same as nearest-neighbor interactions. It is treated in a similar fashion: bonds are put between ghost spin and every lattice spin with a probability $1 - e^{-|h|}$ if $\sigma_g\sigma_i > 0$. After having the bond configuration, we carry out steps (2) and (3) as in zero field, except we do not flip the cluster connected with the ghost spin (we call it a ghost cluster).

The clusters generated by this second version shall be called SW clusters with a ghost spin (SWG) and this is the cluster definition used in this study. Its properties and relations with previous cluster definitions shall be discussed in the next section.

Identification of the clusters is a key step in the implementation of the program. An efficient method has been developed in percolation problems by Hoshen and Kopelman [30]. A simple description can be found in ref. [12], appendix A.3.

3. Clusters in SW algorithm

We now consider the relations between CK clusters and SWG clusters. The joint distribution of spins and consistently chosen bonds is [25]

$$\frac{1}{Z} p^b (1-p)^{dL^d - b} \exp\left\{\sum_\alpha hs_\alpha \eta_\alpha/2\right\}, \tag{4}$$

where Z is the partition function, b is the number of bonds, d is the dimension, s_α is the size of (number of sites belonging to) cluster α, and η_α is the Ising spin for cluster α. Here the clusters are those in the first version of the SW algorithm. The cluster with an Ising spin attached to it will be called the Fortuin–Kasteleyn (FK) cluster of a certain sign. The name CK cluster is reserved only for "−" spin clusters.

Consider summing over all possible bond configurations consistent with a given Ising spin configuration. If a pair of nearest neighbors has the same spins, we have both possibilities: to have a bond or not to have a bond. The sum of these two gives a factor 1. If the two nearest neighbors have opposite spins, there is only one possibility: not to have a bond. Thus this gives the Boltzmann weight for the Ising spin configuration.

Let us express the average number of clusters by the probability of configurations. The number of clusters per site of size s, n_s, is the number of clusters with size s divided by lattice size L^d from a single configuration of a very large system; or looked at differently, sn_s is the probability that a particular site, say the origin, belongs to a cluster of size s. Thus the number of FK clusters with "−" spin is given by

$$sn_s^- = \frac{1}{Z} \sum_{\substack{\text{origin} \in \text{cluster of} \\ \text{size } s \text{ with } \eta_0 = -1}} p^b (1-p)^{dL^d - b} \exp\left\{ \sum_\alpha h s_\alpha \eta_\alpha / 2 \right\}, \tag{5}$$

where η_0 is the Ising spin associated with the origin. Similarly, for FK clusters of "+" spin, we require a summation over bond and spin configurations with the origin belonging to a cluster of size s and with spin $\eta_0 = +1$. We see immediately from eq. (5) the relation

$$n_s = n_s^- \, e^{-hs}. \tag{6}$$

This equation can also be understood from the algorithm without a ghost spin, where each cluster takes "+" or "−" according to the probability $\exp\{h s_\alpha \eta_\alpha / 2\}$.

In the simulation with a ghost spin, if an FK cluster has a negative spin (assuming $h > 0$), it never attaches to the ghost spin, while if an FK cluster has a positive spin, it connects to the ghost spin with a probability $1 - e^{-hs}$. The probability that the cluster α will not connect to the ghost spin is e^{-hs_α}. All negative FK clusters, n_s, are counted as SWG clusters. The positive FK clusters n_s^- are counted only with probability e^{-hs}. Then we have

$$n_s^{\mathrm{SWG}} = n_s + n_s^- \, e^{-hs}, \qquad h > 0. \tag{7}$$

Combining eqs. (6) and (7), we have $n_s^{\mathrm{SWG}} = 2n_s^-$. The SWG cluster number is twice the CK cluster number if $h > 0$. When field is negative, $n_s^{\mathrm{SWG}} = 2n_s^- = 2n_s e^{hs}$. The SWG cluster number is symmetric with respect to field, $n_s^{\mathrm{SWG}}(h) = n_s^{\mathrm{SWG}}(-h)$. One can also express n_s^{SWG} in terms of $n_s^- + n_s$,

$$n_s^{\mathrm{SWG}} = 2 \frac{n_s^- + n_s}{1 + e^{hs}}. \tag{8}$$

This is useful in a Monte Carlo calculation of the number of clusters n_s^{SWG} when $h \neq 0$, using the first version of the algorithm (without ghost spin). Due to the $e^{|hs|}$ enhancing factor, better statistics is obtained. We point out that in zero field n_s^{SWG} is equal to the number of clusters of Hu [18], and is twice the

number of CK clusters. Of course these relations hold only for finite-size clusters.

For an infinite system the origin either belongs to a finite FK cluster of positive spin, or of negative spin, or belongs to an infinite FK cluster. Thus a normalization condition holds,

$$\sum_{s=1}^{\infty} s(n_s^- + n_s^+) + P_\infty = 1 , \tag{9}$$

where P_∞ is the probability that a given site belongs to an infinite FK cluster. The magnetization and susceptibility can be related to the number of clusters. One has (for $h > 0$)

$$m(T, h) = \sum_{s=1}^{\infty} s(n_s^+ - n_s^-) + P_\infty \tag{10a}$$

$$= 1 - \sum_{s=1}^{\infty} s n_s^{\mathrm{SWG}} = P_\infty^{\mathrm{SWG}} . \tag{10b}$$

The last equation is obtained by combining normalization condition (9) and the definition of magnetization (10a). It is also clear from the fact that all finite SWG clusters (excluding the ghost cluster) can assume "+" or "−" spins with equal probability; thus they give zero contributions to the magnetization. The magentization is the same as percolation probability $P_\infty^{\mathrm{SWG}} = \lim_{L\to\infty} L^{-d}\langle s_g \rangle$, where s_g is the size of the ghost cluster. This cluster can have disjoint pieces from the point of view of only lattice spins.

The susceptibility is given by

$$\chi(T, h) = \sum_s s^2 n_s^{\mathrm{SWG}} + L^{-d}(\langle s_g^2 \rangle - \langle s_g \rangle^2) . \tag{11}$$

It is obtained from the same fact that each finite cluster takes "+" or "−" spin with equal probability. For $h = 0$ and $T > T_c$ the ghost cluster fluctuation term vanishes. If $h = 0^+$ and $T < T_c$, one should replace the size of the ghost cluster by the maximum cluster size.

Eqs. (10) and (11) are generalizations of corresponding zero field equations [31, 18, 23]. Alexandrowicz [21] also arrived at eq. (11) from a different point of view.

4. Cluster size distribution

4.1. Scaling around the critical point in zero field

Due to the nature of cluster identification, the algorithm cannot be vectorized efficiently. The simulation was done on an IBM 3090 computer without

vector feature, with a speed of 3 to 4 microseconds per Monte Carlo step (MCS) per spin. The total computer time used in this work is about 400 hours. Most of our data are taken from a cubic system of linear size $L = 98$, with a run of 10^3 to 10^4 MCS/spin, discarding the first 400 MCS/spin. Notice that a maximum correlation time one can have in such a system is $L^{0.75} \approx 30$ [19]. This should be compared with a correlation time of order $L^2 \approx 10^4$ using a single-spin-flip algorithm [32].

In this section we omit the superscript SWG for the number of clusters. Scaling theory [9, 16] asserts for the number of clusters, in the limit of small $\varepsilon = |T - T_c|/T_c$, small field h, and large cluster size s,

$$n_s(\varepsilon, h) \simeq s^{-\tau}\tilde{n}(\varepsilon s^{\sigma}, hs) , \tag{12}$$

where τ and σ are related to thermal exponents γ and β by $\tau = 2 + \beta/(\gamma + \beta)$, $\sigma = 1/(\gamma + \beta)$ [3].

Right at the critical point the number of clusters should go asymptotically as $s^{-\tau}$. Fig. 1 is a plot of number of clusters n_s vs. size s in $\log_{10}$ scale. (For earlier data, see ref. [33], fig. 2 and ref. [31], fig. 8.) We see a nice straight line,

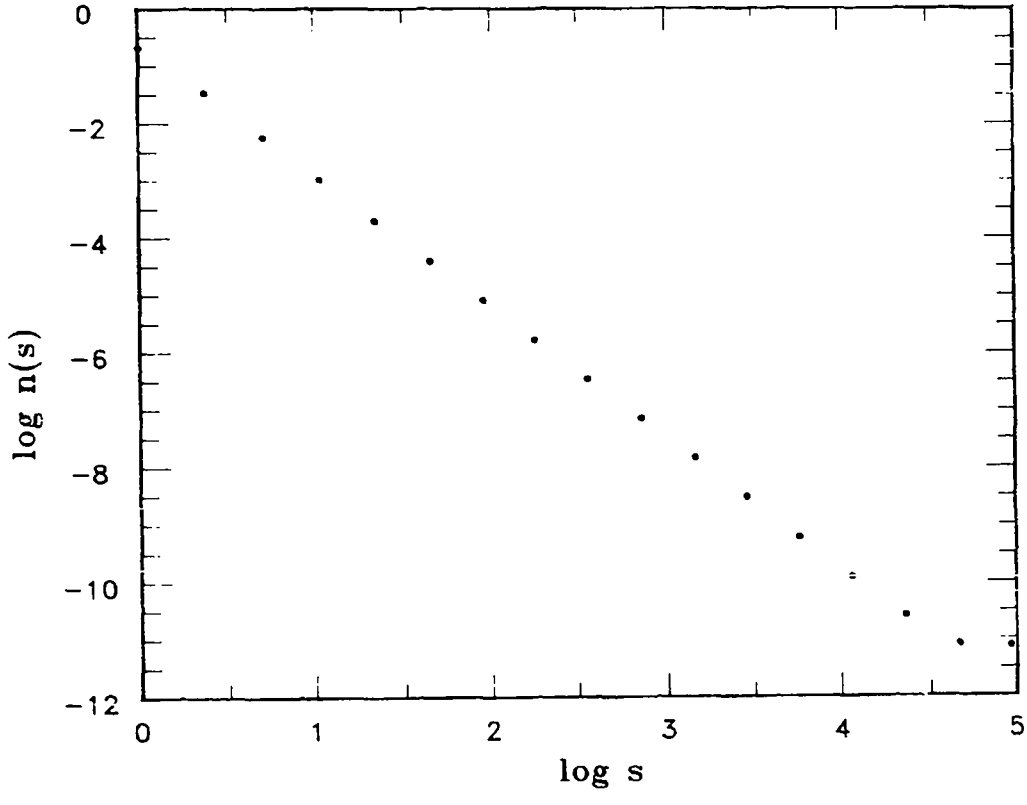

Fig. 1. Number of clusters n_s vs. size s in $\log_{10}$ scale at the critical point $T = T_c$, $h = 0$, for a cubic system of linear size $L = 98$. The slope of a straight-line-fit gives an effective value $\tau = 2.27$.

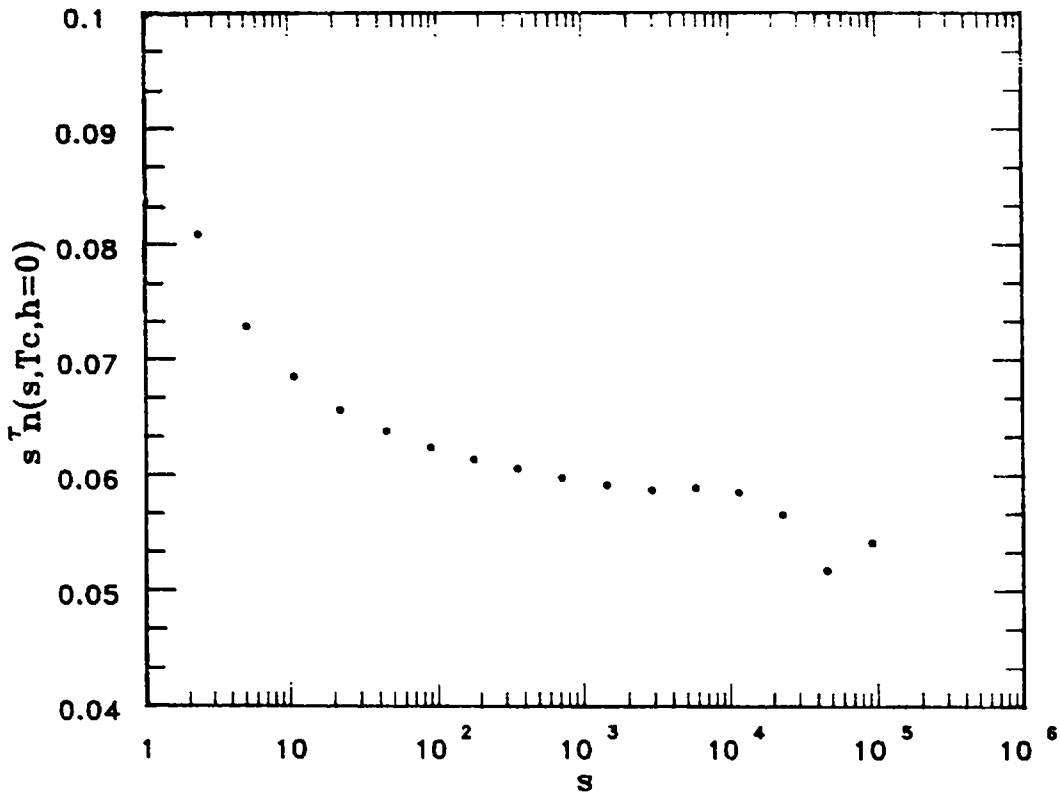

Fig. 2. Number of clusters at the critical point plotted as $s^{\tau}n_s$ vs. s for the two-dimensional nearest-neighbor Ising model of a 950×950 system, where $\tau = 31/15$.

indicating an algebraic decay of the number of clusters with size. However, careful inspection of the data reveals deviation from eq. (12). An accurate estimate from our data for the exponent τ is hampered due to a correction to scaling for small s and due to a finite-size effect for large s. Using data in the range $4 < s < 64$ from sizes $L = 32$, 59 and 64, where the finite-size effect is small, one would get a value 4% higher than the best known value $\tau \approx 2.21$ [34] (through scaling relation $\tau = 2 + \beta/(\gamma + \beta)$). With size $L = 98$, a trend of decreasing τ is clearly seen. This difficulty is also present in random percolation even for a very large system [35].

To check whether the asymptotic value can really be reached for large systems, we investigated a two-dimensional Ising model (for a finite-size scaling analysis of this system, see ref. [23]). Indeed, for a system of 950×950, effective τ agrees with its theoretical value within less than 1 per cent deviation for $10^3 < s < 10^4$. The finite-size effect becomes severe for $s > 10^4$. In fig. 2 we plotted $s^{\tau}n_s$ vs. s. A flat part is just beginning to appear for $s > 10^5$. It is not yet seen with size 512×512. Data on fig. 2 could be fitted to $cs^{-\tau}(1 + as^{-\Omega})$ with a correction-to-scaling exponent $\Omega = 0.43$ and the theoretical value of τ.

We now consider the cluster number near the critical point in zero field. If scaling holds, curves $s^{\tau}n_s$ vs. εs^{σ} for different ε should collapse onto a single

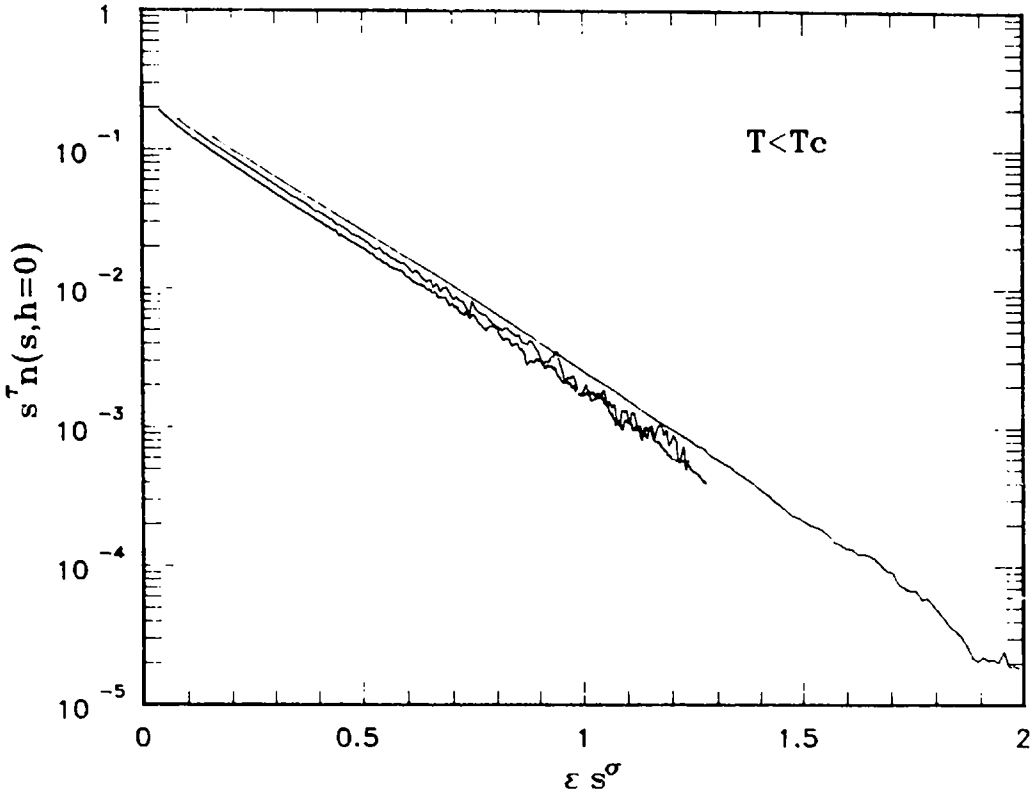

Fig. 3. Semi-logarithmic plot of $s^\tau n_s$ vs. εs^σ below T_c in zero field, for $\varepsilon = |T - T_c|/T_c = 0.025$, 0.05 and 0.1, from bottom to top, respectively, where $\tau = 2.2075$, $\sigma = 0.640$. The data points are connected by straight lines. For large s the data have been averaged over a small interval.

scaling curve. Fig. 3 is such a plot for temperatures below T_c, with $\varepsilon = 0.025$, 0.05 and 0.1, respectively. Systematic deviation from scaling due to finite ε is clearly seen. However our data suggest, as $\varepsilon \to 0$, a limiting scaling curve will be achieved.

The curves in fig. 3 look quite straight for $\varepsilon s^\sigma > 0.5$. Thus it is consistent with $\ln(s^\tau n_s) \simeq -\Gamma s^{2/3}$ (for given ε); since $\sigma \approx 0.640$, it is indistinguishable from 2/3 from our data. Such a "surface" term is known to be present at low temperatures [36, 37,33]. Our data are consistent with the presence of a surface term up to the critical point, with a "surface tension" vanishing as $\varepsilon^{2-3\sigma}$. The surface tension Γ that appears here differs from the normal surface tension which vanishes as $\varepsilon^{2\nu}$ [38]. The limiting scaling curve should behave as $\ln \tilde{n}(x) \propto -x^{2-3\sigma}$ for large $x = \varepsilon s^\sigma$ in order to be consistent with this $s^{2/3}$ dependence.

Fig. 4 is a plot of $s^\tau n_s$ vs. $\varepsilon^{1/\sigma} s$ for $T > T_c$. Systematic deviation is also observed for small s. Different ε curves overlap better for large s. In this semi-logarithmic plot of $s^\tau n_s$ against linear s, we have a straight line with a slight curvature for large s. An exponential decay is expected for large s above the critical temperature.

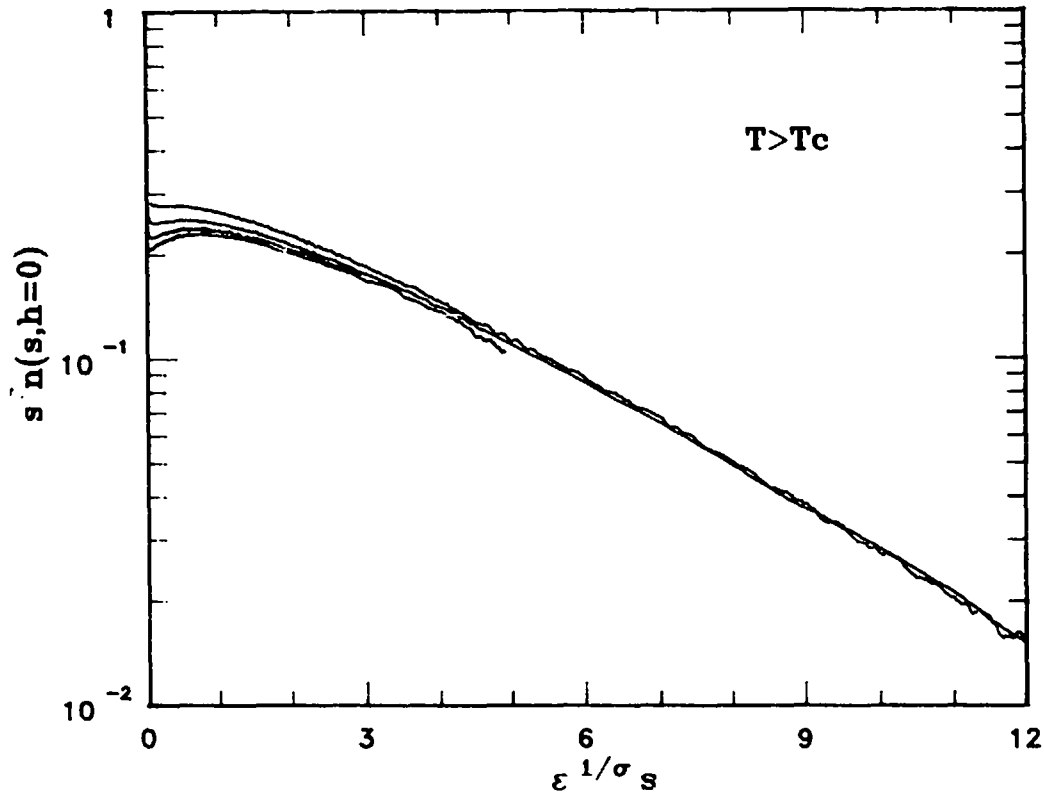

Fig. 4. Semi-logarithmic plot of $s^{\tau}n_s$ vs. $\varepsilon^{1/\sigma}s$ above T_c in zero field, where ε takes value 0.0125, 0.025, 0.05 and 0.1, from bottom to top, respectively.

In contrast to $T < T_c$ with a monotonic decreasing scaling function, a maximum around $\varepsilon^{1/\sigma} \approx 0.7$ is observed for $T > T_c$. This feature and different large s behavior below and above T_c are quite similar to random percolation [35].

4.2. Scaling in a magnetic field

Fig. 5 is a semi-logarithmic plot of $s^{\tau}n_s$ as a function of cluster size s for values of field $h = 0.01$, 0.02, and 0.1, at $T = T_c$. Strong curvature is present. The data can not be described by a simple exponential decay as in Fisher droplet model eq. (1), where the surface term is supposed to vanish for $T = T_c$. Fig. 6 is a scaling plot with the scaling variable hs. There are systematic deviations from scaling due to finite h. In the limit h goes to zero and s goes to infinity we expect that a scaling curve will be reached.

It is expected from rigorous argument [39] that the number of clusters go as e^{-hs} plus terms independent of h, for sufficiently large field h and large size s, for all temperatures. Our data are clearly not in this limit yet. We plotted in fig. 7 the local slope $-\mathrm{d}(\ln s^{\tau}n_s)/\mathrm{d}(hs)$ as a function of $(hs)^{1/3}$ (taking the

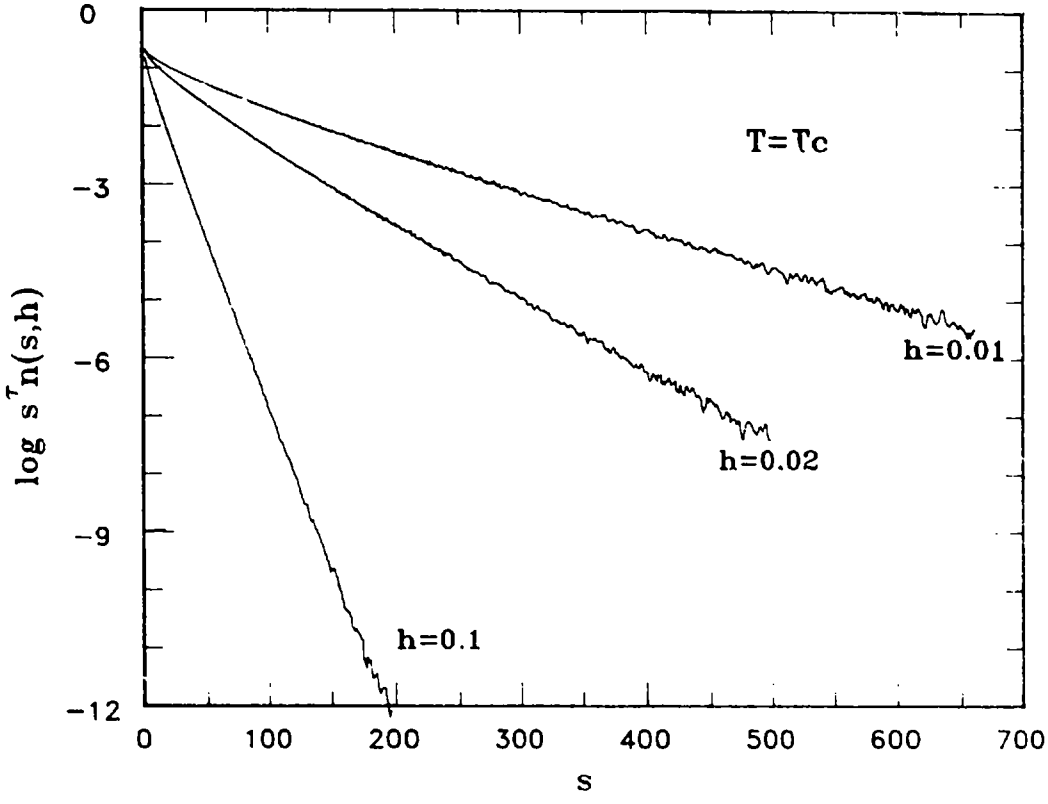

Fig. 5. Number of clusters plotted as $\log_{10} s^{\tau} n_s$ vs. s for different values of h at $T = T_c$. The exponent $\tau = 2.2075$ is used.

curve $h = 0.02$). The slope decreases from 2.8 to 1.4 within the range of our data. A previous study [31] was not able to see this hs dependence due to small hs values. We expect that the slope approaches to 1 for large hs. It is a delicate question whether $s^{\tau} n_s$ will approach e^{-hs} eventually as hs goes to infinite based only on numerical data. Depending on how the limit is approached, the final value could be 1 or 1.3. If one assumes that a surface term $s^{2/3}$ is present, one should have a $s^{-1/3}$ correction to the slope. We indeed have a trend of approaching to 1. On the other hand, we have a curvature. An empirical $s^{-2/3}$ correction to the slope gives a straighter line, with a limit around 1.3. We shall argue in the next section that one must have a $s^{2/3}$ dependence in the number of clusters. A final value is presumably 1 instead of 1.3.

4.3. Number of clusters away from the critical point

If we consider n_s^+ with $h > 0$, such clusters percolate on a line. The percolation transition is supposed to be in the same universality class as random percolation except at $h = 0$ where it takes Ising critical exponents [13]. In random percolation [40] as well as in quite general correlated percolation

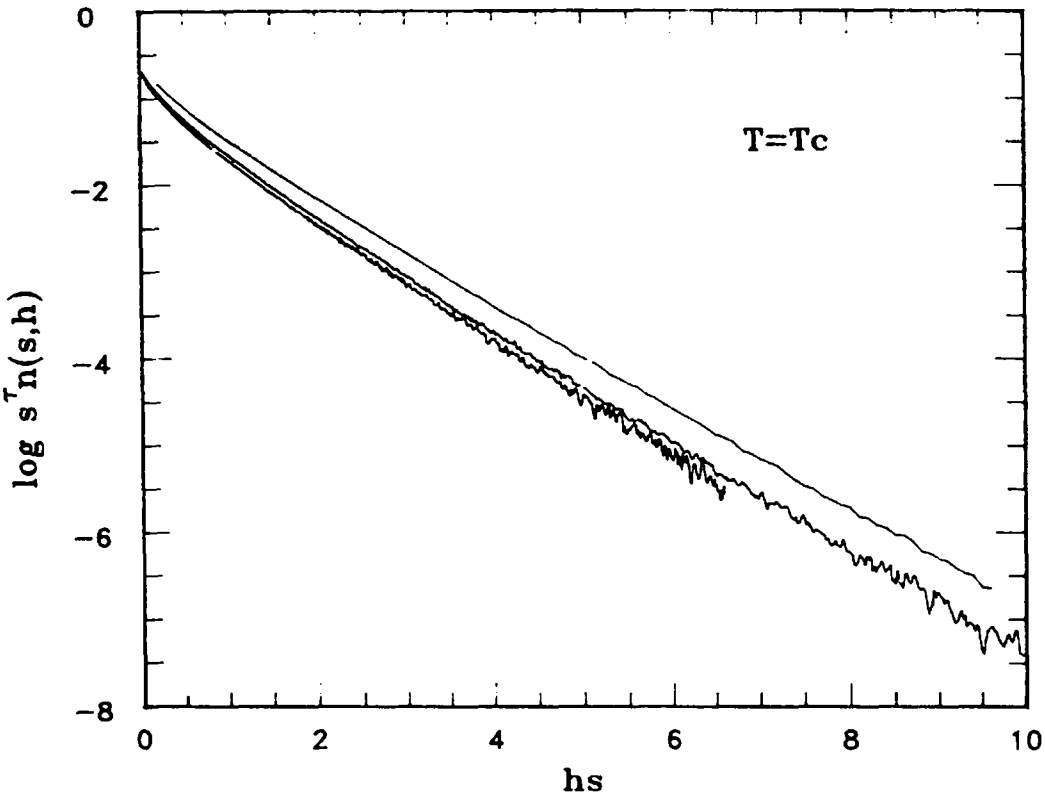

Fig. 6. The same set of data as in fig. 5 plotted in scaling variable hs. $h = 0.01$, 0.02 and 0.1, from bottom to top, respectively.

[36, 37] the number of clusters (in d dimensions) in the large s limit is bounded by

$$n_s^+ > e^{-\Gamma s^{(d-1)/d}}, \tag{13}$$

whenever the system has an infinite percolating cluster. At sufficiently low temperatures, the inequality becomes an equality from rigorous argument and this equality probably also holds up to the percolation threshold from numerical results [12] for random percolation (corresponding to $h = \infty$). We assume that the equality holds also for finite h up to percolation threshold. Using eq. (6), (7) and (13), we see that n_s is

$$\ln n_s \simeq -hs - \Gamma(T, h)s^{2/3}, \qquad h \geq 0, \tag{14}$$

for sufficiently large s below the CK cluster percolation line $h = \pm\tilde{h}(T)$. Notice that we do not require h large. In fact eq. (14) is verified numerically for $h = 0$ at $T/T_c = 0.8$ [33] and certainly is the case for $h = \infty$, since it is just a random bond percolation. On the percolation line $\pm\tilde{h}(T)$ we have $n_s \propto s^{-\tau} e^{-hs}$, where

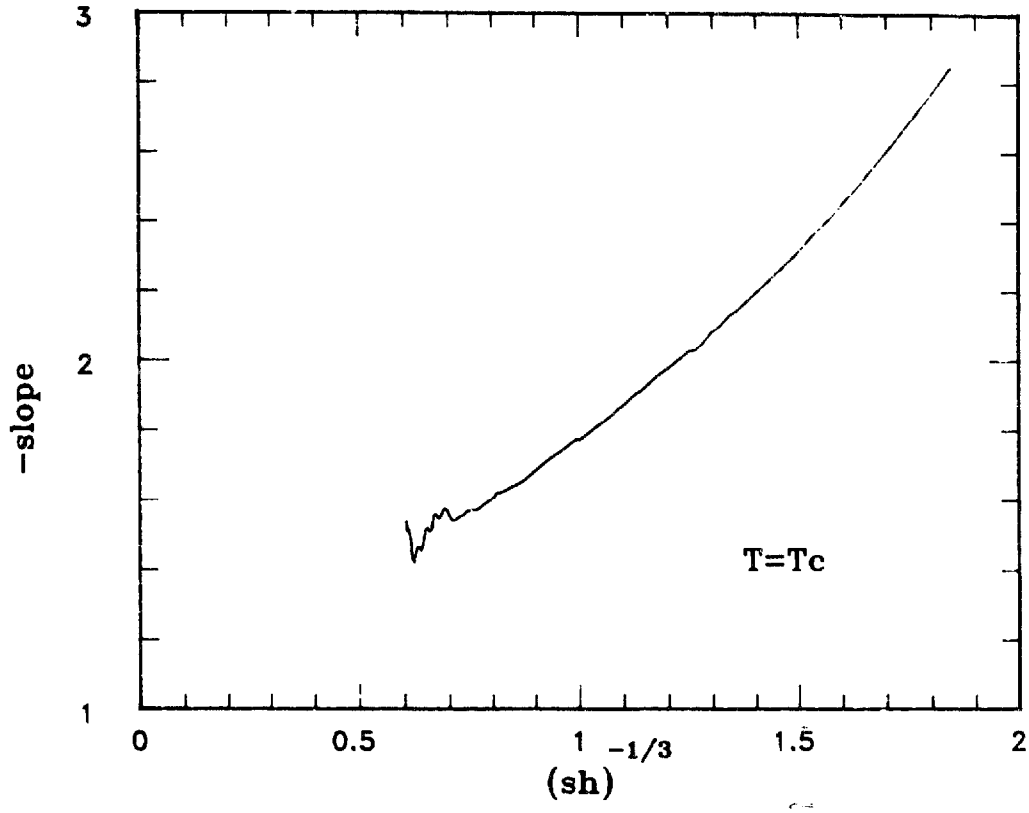

Fig. 7. Local slope ($h = 0.02$) in fig. 6 plotted against $(hs)^{1/3}$.

$\tau_p \approx 2.2$ is the random percolation exponent. One expects a simple exponential decay $n_s \propto e^{-(h+c)s}$ for large s on the high temperature side of the percolation line. A possible consequence of the disappearance of the surface term on the percolation line is discussed in ref. [22].

In connection with the scaling hypothesis of the number of clusters, eq. (12), near the critical point, we must require that eq. (14) has a correct scaling form near $\varepsilon = 0$ and $h = 0$. We thus propose

$$\Gamma(T, h) \simeq h^{2/3} \tilde{\Gamma}(\varepsilon / h^{\sigma}) . \tag{15}$$

The above equation is supposed to be valid on the low temperature side of the percolation line. In particular we must require that $\tilde{\Gamma}(x)$ equals zero on the percolation line $\pm \tilde{h}(\varepsilon)$. This can happen for a specific value of the scaling argument $x_0 = \varepsilon / h^{\sigma}$. Such a reasoning then leads to a prediction for the percolation line near the critical point,

$$h = \pm \tilde{h}(\varepsilon) \propto \varepsilon^{1/\sigma} . \tag{16}$$

We now look at numerical results. Fig. 8 is a plot of the number of clusters

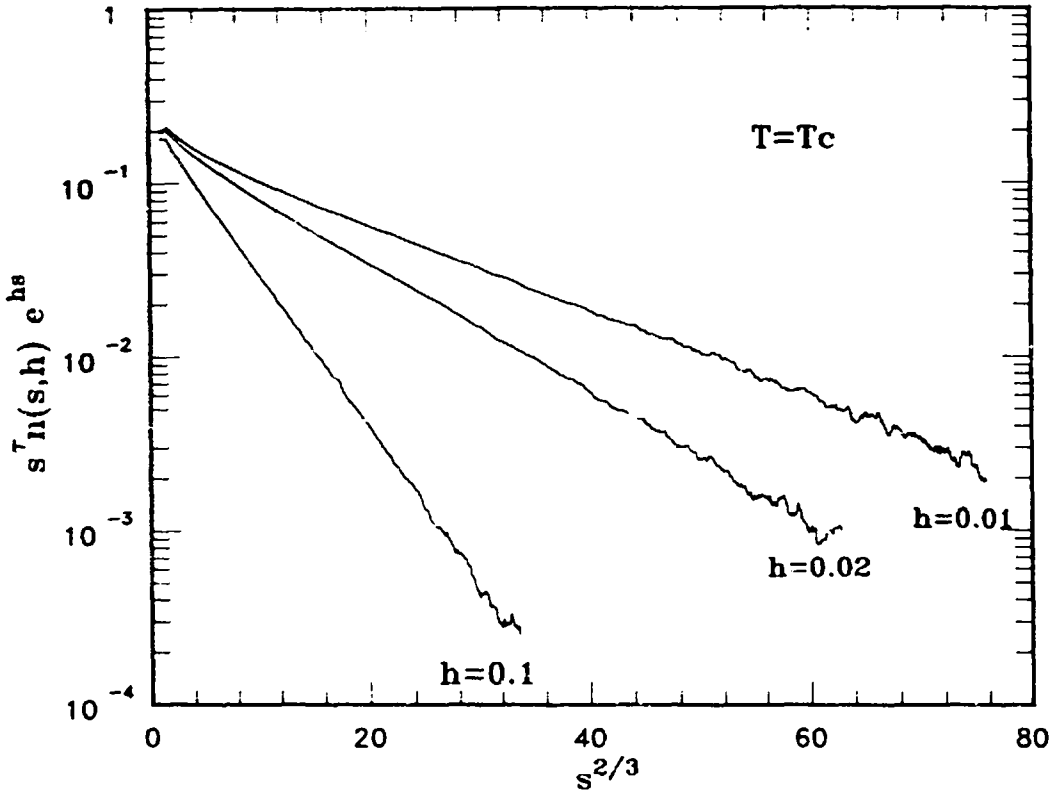

Fig. 8. Same set of data as in fig. 5 or fig. 6 plotted as $s^{\tau} e^{hs} n_s$ vs. $s^{2/3}$.

divided by a factor $s^{-\tau} e^{-hs}$ vs. $s^{2/3}$ at $T = T_c$ for values of $h = 0.01$, 0.02 and 0.1. According to eq. (14) we should have straight lines in such a plot for large s. This is indeed convincingly the case. A plot against s shows the curvature.

Figs. 9a and b are similar plots as fig. 8 at low temperature, large field ($T/T_c = 0.82$, $h = 1$), and above the critical temperature, large field ($T/T_c = 1.1$, $h = 2$), but in the CK cluster percolating region. The latter plot has some curvature. They can be consistent with $s^{2/3}$ dependence. A power-law factor $s^{-\tau}$ seems needed in order to have clear straight lines in these plots.

We investigated the cluster number 5 percent below and above T_c. Fig. 10a is the number of clusters ratio between $h \neq 0$ and $h = 0$ for $T/T_c = 0.95$ (see ref. [31], fig. 11, for previous data). Again, a slight curvature is observed. Fig. 10b is a "scaling" plot. In principle the ratio of the number of clusters will not scale as hs when $T \neq T_c$. However, if $\Gamma(T, h)$ in eq. (14) has a weak dependence on h, such scaling is expected. This is probably so, since $\Gamma(T, h)$ approaches non-zero value as $h \to 0$, $T < T_c$. Data scale for $h = 0.02$, 0.05 and 0.1. For large h and s the leading term should go as e^{-hs}. Our data indicate that such behavior could be approached very slowly at $T/T_c = 0.95$. This is due to a $s^{2/3}$ correction. Such $s^{2/3}$ behavior is also observed from a plot similar to fig. 8.

Fig. 11 is the result 5 percent above T_c, where we have a nice exponential

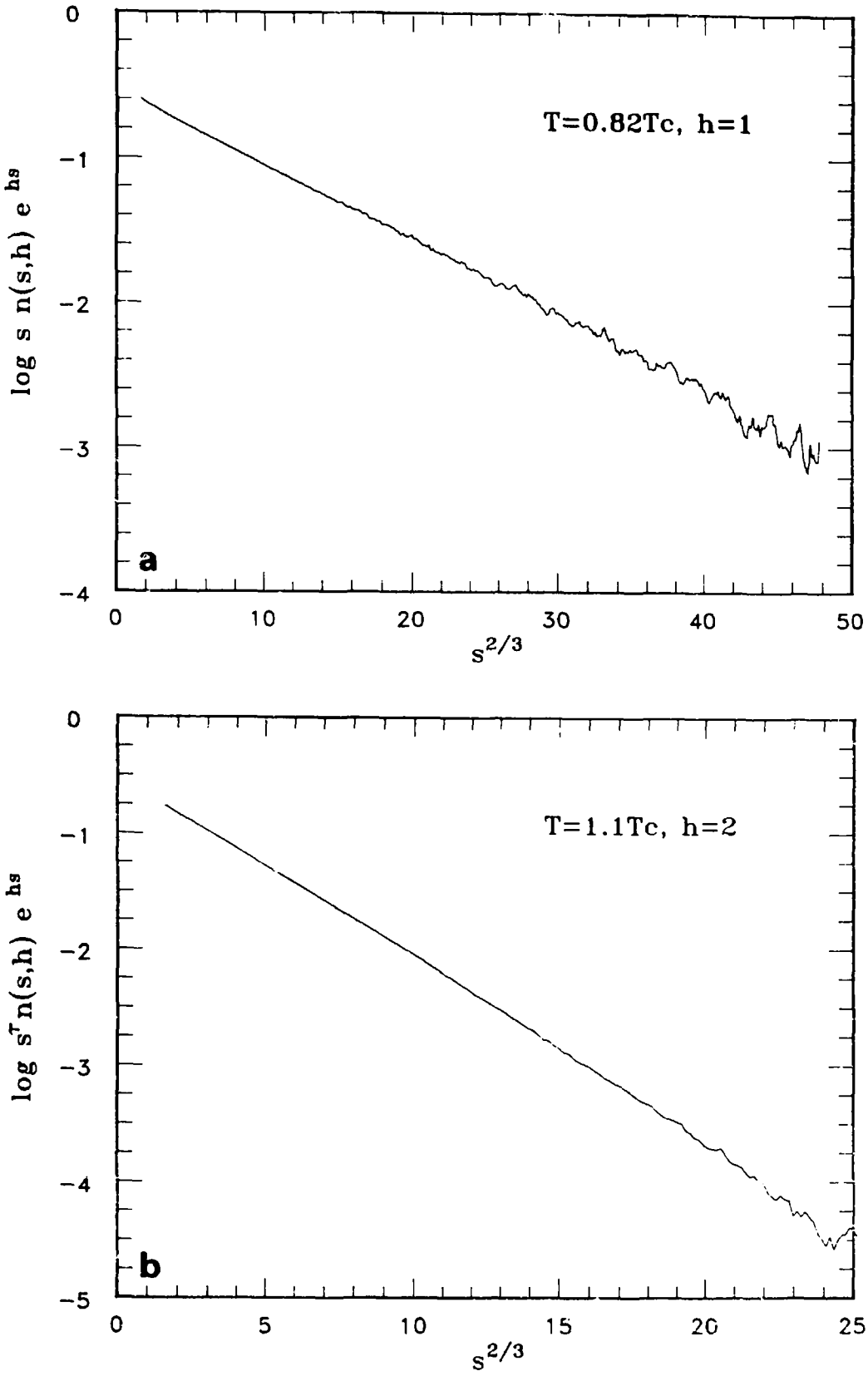

Fig. 9. Number of clusters plotted as $\log_{10} s^{\tau} e^{hs} n_s$ vs. $s^{2/3}$ at: (a) $T/T_c = 0.82$, $h = 1$; (b) $T/T_c = 1.1$, $h = 2$.

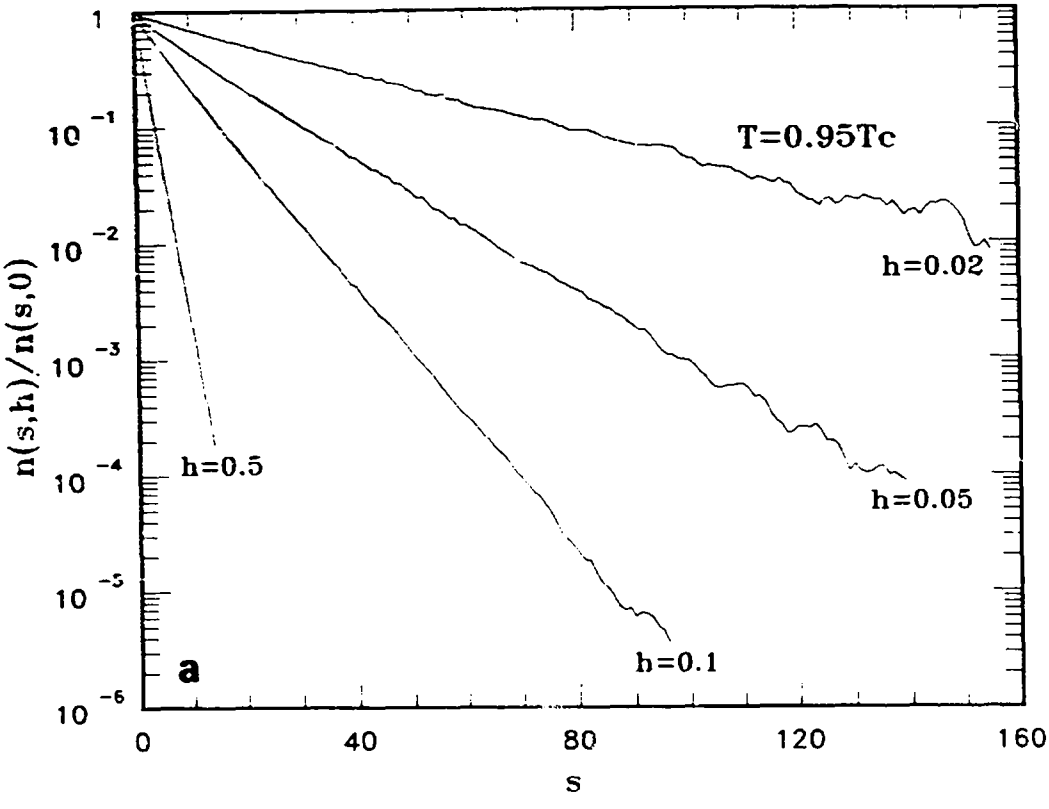

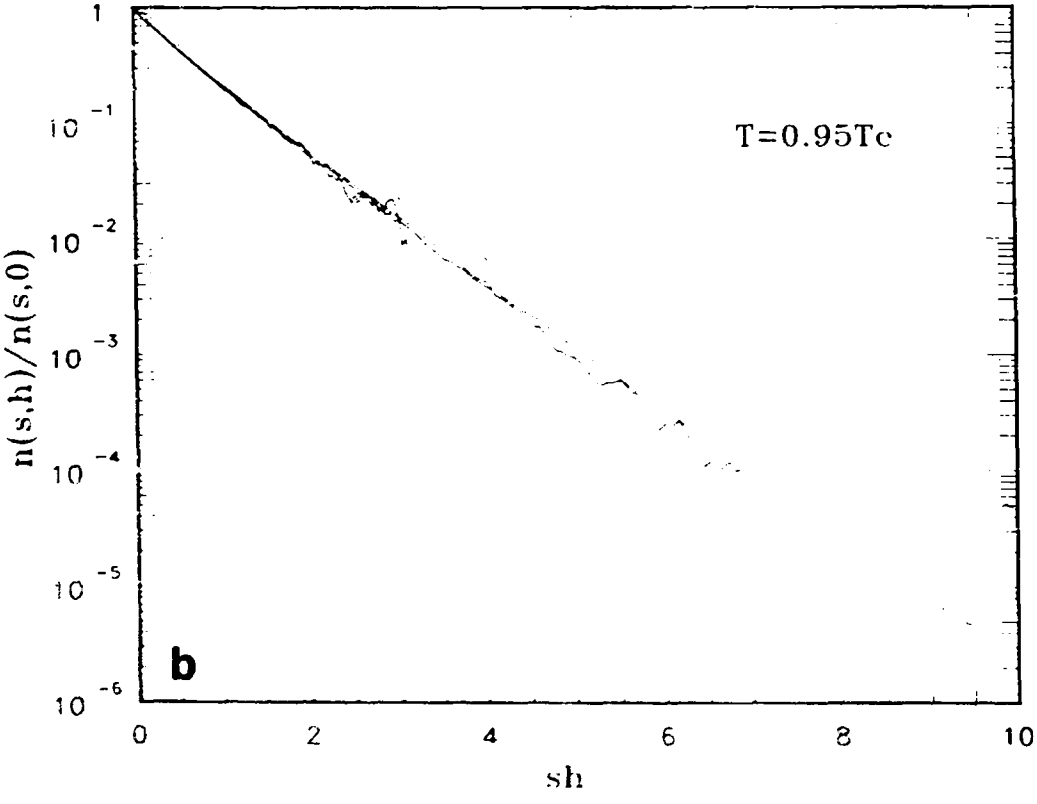

Fig. 10. Ratio of number of clusters between $h \neq 0$ and $h = 0$ at $T/T_c = 0.95$: (a) plotted against s; (b) plotted against sh. The straight line is e

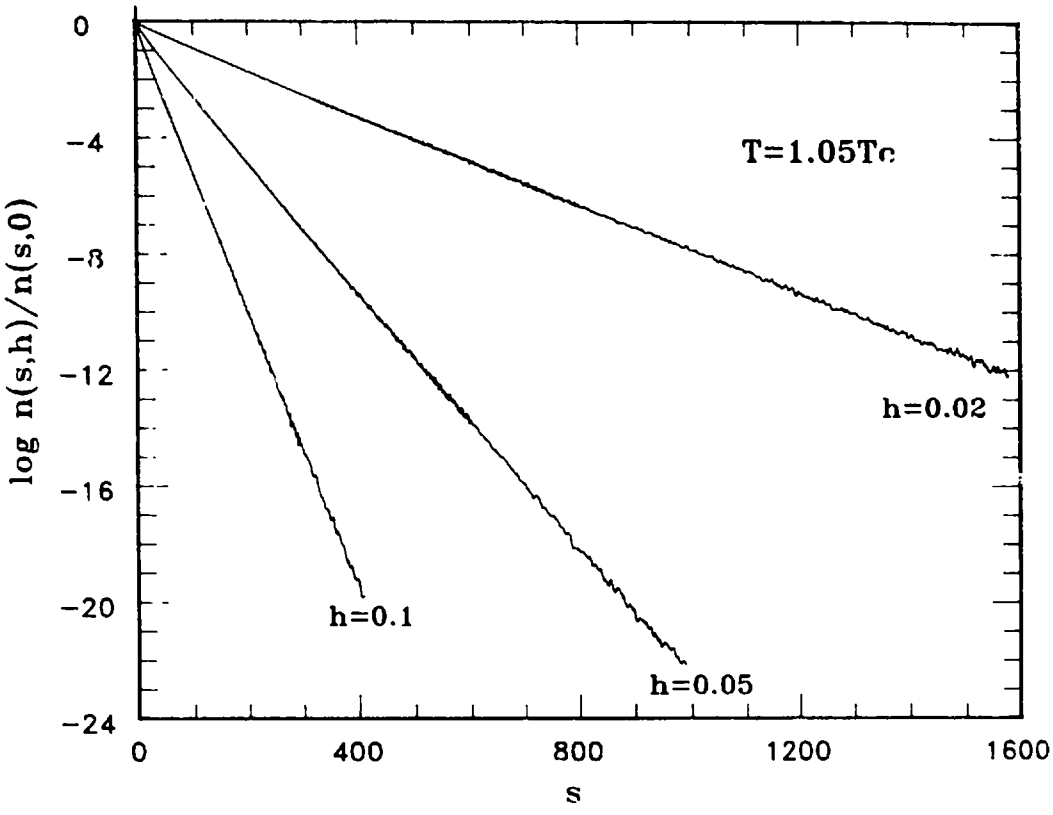

Fig. 11. Ratio of number of clusters between $h \neq 0$ and $h = 0$ at $T/T_c = 1.05$ plotted as $\log_{10}(n_s(h)/n_s(0))$ against s.

decay over many order of magnitudes without any need for an $s^{2/3}$ term. We have used eq. (8) to calculate the number of clusters. With a straight definition, we could only get reliable data with maxima s a factor 4 to 5 smaller. The data do not scale, if plotted against hs.

5. Percolation line near the critical point

We locate the percolation transition line by looking at the peak of the second moment of the number of clusters n_s^+, excluding the largest cluster. According to our discussion in the previous section, the percolation line behaves asymptotically as $h \propto \varepsilon^{1/\sigma}$ for small ε. We plotted h vs. ε in log–log scale in fig. 12. The straight line has a slope corresponding to $1/\sigma = 1.56$. The data for $\varepsilon > 0.04$ give a curvature with decreasing slope as ε decreases. The data for $\varepsilon \leq 0.04$ are consistent with the theoretical prediction within errors.

Because the line $\varepsilon = 0$ is perpendicular to the percolation line $h \propto \varepsilon^{1/\sigma}$ ($1/\sigma > 1$), we do not have a problem of crossover to random percolation. This enabled us to see clearly the $s^{2/3}$ effect in fig. 8.

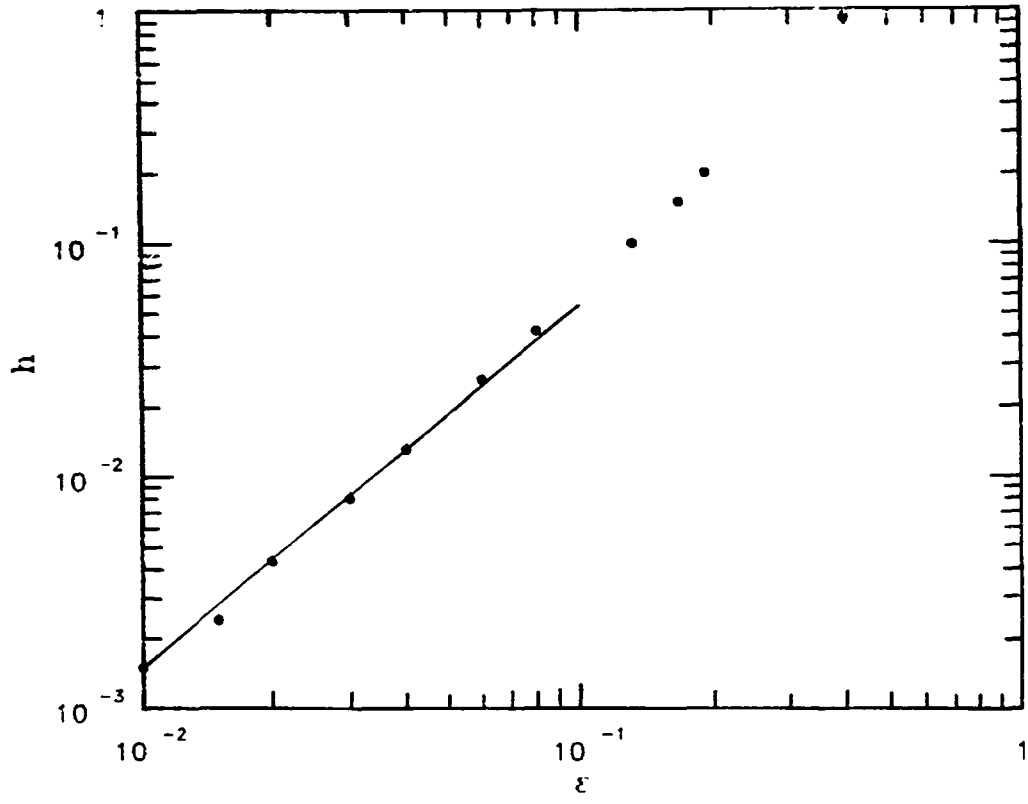

Fig. 12. Percolation transition line h vs. ε near the critical point. The straight line has a slope $1/\sigma = 1.56$. A least-squares fit using data $\varepsilon < 0.04$ gives a slope 1.54 ± 0.04.

6. Conclusion

We investigated the clusters in the SW algorithm with a ghost spin. Such definition of clusters is symmetric in the field h for finite clusters. With this definition, the magnetization is equal to the percolation probability of the corresponding clusters. The number of clusters is related to that of Coniglio and Klein by a factor 2 in the $h > 0$ part of the $(h-T)$ phase diagram and by $2e^{-|h|s}$ for the $h < 0$ part of the phase diagram. In so doing, a percolation transition line of the CK clusters is suppressed. However, the effect is still present in a surface term dependence of the number of clusters. Our Monte Carlo data are consistent with such dependence.

In connection with the Fisher droplet model, the scaling structure of the number of clusters n_s is preserved. But instead of a simple temperature dependence $\Gamma \propto \varepsilon$ as in eq. (1), it is modified to $\Gamma = h^{2-\tau}\tilde{\Gamma}(\varepsilon/h^{\sigma})$. The surface term, instead of vanishing on the line $\varepsilon = 0$ as in the Fisher droplet model, vanishes on the curve $h = \pm\tilde{h}(\varepsilon) \propto \varepsilon^{1/\sigma}$. Because of a field dependence in the surface term, it is not possible to write the free energy of the Ising model (or singular part of it) as a sum of the number of clusters. In addition, the

susceptibility has an infinite-cluster fluctuation term. Our simulations were able to confirm many old concepts of the droplet model due to a better definition of clusters, a better algorithm at $T = T_c$, and more computer time.

Acknowledgements

The author thanks D. Stauffer for suggesting the problem and K. Binder, R.B. Griffiths, D.W. Heermann, J. Kertész and P. Lauwers for stimulating discussions. He thanks D. Chowdhury for a critical reading of the manuscript.

Note added in proof

A. Coniglio, F. di Liberto, G. Monroy and F. Peruggi (J. Phys. A Lett., in press) employ the same definition of clusters using a ghost spin. Relations between clusters and thermodynamic quantities are discussed. Alexandrowicz's spin blocks differ from our definition of clusters, while his number of clusters agree with our number of clusters (ref. [21], note added in proof). P. Lauwers and V. Rittenberg (submitted to Phys. Lett.) simulated the 2D Ising model in a field without the use of a ghost spin. See also P. Tamayo, R.C. Brower and W. Klein (preprint), U. Wolff (preprint) and D.W. Heermann and A.N. Burkitt (Physica A, in press) concerning the dynamical aspects of the cluster-flip algorithms.

References

[1] J.E. Mayer, J. Chem. Phys. 5 (1937) 67.
[2] W. Band, J. Chem. Phys. 7 (1939) 324, 927.
T.P. Tseng, S.K. Feng, C. Ch'eng and W. Band, J. Chem. Phys. 8 (1940) 20.
C. Ch'eng, T.P. Tseng, S.K. Feng and W. Band, J. Chem. Phys. 9 (1941) 123.
[3] M.E. Fisher, Physics 3 (1967) 255.
[4] C.S. Kiang, Phys. Rev. Lett. 24 (1970) 47.
[5] C.S. Kiang and D. Stauffer, Z. Phys. 235 (1970) 130.
A. Eggington, C.S. Kiang, D. Stauffer and G.H. Walker, Phys. Rev. Lett. 26 (1971) 820.
D. Stauffer, C.S. Kiang and G.H. Walker, J. Stat. Phys. 3 (1971) 323.
D. Stauffer, C.S. Kiang, G. H. Walker, O. Puri, J. Wise and E. Patterson, Phys. Lett. A 35 (1971) 172.
[6] F.F. Abraham, Homogeneous Nucleation Theory (Academic Press, New York, 1974).
K. Binder and D. Stauffer, Adv. Phys. 25 (1976) 345.
[7] H. Müller-Krumbhaar, Phys. Lett. A 48 (1974) 459.
[8] E. Stoll, K. Binder and T. Schneider, Phys. Rev. B 6 (1972) 2777.
[9] H. Müller-Krumbhaar and E.P. Stoll, J. Chem. Phys. 65 (1976) 4294.

[10] H. Müller-Krumbhaar, in: Monte Carlo Methods in Statistical Physics, K. Binder, ed. (Springer, Heidelberg, 1979).
[11] D.W. Heermann and D. Stauffer, Z. Physik B 44 (1981) 339.
[12] D. Stauffer, Introduction to Percolation Theory (Taylor and Francis, London, 1985).
[13] A. Coniglio and W. Klein, J. Phys. A 13 (1980) 2775.
[14] M.F. Sykes and D.S. Gaunt, J. Phys. A 9 (1976) 2131.
[15] A.L. Stella and C. Vanderzande, Phys. Rev. Lett. 62 (1989) 1067.
[16] K. Binder, Ann. Phys. 98 (1976) 390.
[17] P.W. Kasteleyn and C.M. Fortuin, J. Phys. Soc. Jpn. Suppl. 26 (1969) 11.
C.M. Fortuin and P.W. Kasteleyn, Physica (Utrecht) 57 (1972) 536.
[18] C.-K. Hu, Phys. Rev. B 29 (1984) 5103.
[19] R.H. Swendsen and J.-S. Wang, Phys. Rev. Lett. 58 (1987) 86.
[20] A. Coniglio, H.E. Stanley and W. Klein, Phys. Rev. Lett. 42 (1979) 518.
[21] Z. Alexandrowicz, Physica A 160 (1989) 310.
[22] J. Kertész, Physica A 161 (1989) 58, this volume.
[23] M.D. De Meo, D.W. Heermann and K. Binder, J. Stat. Phys. (1989), to be published.
[24] D. Kandel, E. Domany, D. Ron, A. Brandt and E. Loh, Jr., Phys. Rev. Lett. 60 (1988) 1591.
[25] R.G. Edwards and A.D. Sokal, Phys. Rev. D 38 (1988) 2009.
[26] U. Wolff, Phys. Rev. Lett. 60 (1988) 1461; 62 (1989) 361.
[27] F. Niedermayer, Phys. Rev. Lett. 61 (1988) 2026.
[28] R.C. Brower and P. Tamayo, Phys. Rev. Lett. 62 (1989) 1087.
[29] J.-S. Wang, R.H. Swendsen and R. Kotecký, Phys. Rev. Lett. 63 (1989) 109.
[30] J. Hoshen and R. Kopelman, Phys. Rev. B 14 (1976) 3438.
[31] J. Kertész, D. Stauffer and A. Coniglio, in: Percolation Structures and Processes, G. Deutscher, R. Zallen and J. Adler, eds. (Hilger, Bristol, 1983), p. 121.
[32] S. Wansleben and D.P. Landau, J. Appl. Phys. 61 (1987) 3968.
[33] J. Roussenq, A. Coniglio and D. Stauffer, J. Phys. (Paris) 43 (1982) L 703.
[34] J. Zinn-Justin, J. Phys. (Paris) 42 (1981) 783.
G.S. Pawley, R.H. Swendsen, D.J. Wallace and K.G. Wilson, Phys. Rev. B 29 (1984) 4030.
M.E. Fisher and J.-H. Chen, J. Phys. (Paris) 46 (1985) 1645.
[35] D. Stauffer, Phys. Rep. 54 (1979) 1.
[36] M. Aizenman, F. Delyon and B. Souillard, J. Stat. Phys. 23 (1980) 267.
[37] F. Delyon, B. Souillard and D. Stauffer, J. Phys. A 14 (1981) L 243.
[38] B. Widom, in: Phase Transitions and Critical Phenomena, vol. 2, C. Domb and M.S. Green, eds. (Academic Press, London, New York, 1972), p. 79.
[39] B. Souillard and J. Imbrie, cited by Kertész et al. [31] as private communication.
[40] H. Kunz and B. Souillard, Phys. Rev. Lett. 40 (1978) 133; J. Stat. Phys. 19 (1978) 77.